Australia's National Science Agency
www.csiro.au

Remotely sensed time-series (2000–2018) estimation of evapotranspiration in the Indus Basin

Implementation, evaluation and analysis

Jorge L. Peña-Arancibia, Mobin-ud Din Ahmad, Mac Kirby and Muhammad J.M. Cheema

February 2020

Australian Government

Australian Aid

Citation

Peña-Arancibia JL, Ahmad MD, Kirby JM and Cheema MJM (2020) Remotely sensed time-series (2000–2018) estimation of evapotranspiration in the Indus Basin: Implementation, evaluation and analysis. Sustainable Development Investment Portfolio (SDIP) project. CSIRO, Australia. 34 pp

Author affiliations

Jorge L. Peña-Arancibia and Mobin D. Ahmad are research scientists at CSIRO Land and Water, Canberra, Australia.

Mac Kirby is a visiting research scientist at CSIRO Land and Water, Canberra.

Muhammad J.M. Cheema is an Associate Professor at University of Agriculture Faisalabad.

Copyright

Important disclaimer

Ethics

The activities reported herein have been conducted in accordance with CSIRO Social Science Human Research Ethics approval 011/17.

This report designed and implemented by CSIRO contributes to the South Asia Sustainable Development Investment Portfolio and is supported by the Australian aid program. Further details on CSIRO SDIP projects are available from http://research.csiro.au/sdip.

SDIP's goal is increased water, food and energy security in South Asia to support climate resilient livelihoods and economic growth, benefiting the poor and vulnerable, particularly women and girls

SDIP 2020 objective: Key actors are using and sharing evidence, and facilitating private sector engagement, to improve the integrated management of water, energy and food across two or more countries - addressing gender and climate change.

All CSIRO SDIP projects consider gender. In this report we have assumed that an improved, quantitative understanding of spatial evapotranspiration is of benefit to all, regardless of gender and other social factors. Excluding gender analysis, however, can lead to 'gender blind' tools, findings and decisions that reinforce existing gender inequities. This gap should be borne in mind when interpreting this report, and any application of its findings will need to integrate gender-specific and other social considerations to ensure benefits are distributed equitably.

Contents

Figures

Tables

Acknowledgments

We would like to acknowledge the support of the Government of Australia through its Department of Foreign Affairs and Trade (DFAT) in financing this study. We also thank the Australian High Commission in Islamabad, the Pakistan High Commission in Canberra and Dr John Dore (DFAT Sustainable Development Investment Portfolio (SDIP) adviser) and Ms Paula Richardson (DFAT SDIP coordinator) for their active engagement in the project. We would like to thank the Pakistan Ministry of Water Resources and provincial irrigation departments for their interest, advice and support, including the provision of data and expertise, hosting the project team on field visits, and provision of guidance throughout the project.

We would also like to acknowledge Dr Bakhshal Khan Lashari, Dr Arjumand Zehra Zaidi and Mr Nabeel Ali Khan from USPCAS-W at Mehran University of Engineering & Technology, for discussions and their contributions.

Dong Dong Kong (Sun-Yat Sen University) and Catherine Ticehurst (CSIRO Land and Water) are gratefully acknowledged for their support with Google Earth Engine.

Dr Juan Pablo Guerschman and Susan Cuddy (CSIRO Land and Water) are acknowledged for revising the report, which improved its quality and content.

Executive summary

Evapotranspiration is the largest water balance component in semi-arid irrigated systems. The Indus Basin Irrigation System (IBIS, ~140,000 km^2) is the largest irrigated system in the world. Remote sensing can provide consistent and robust spatial estimates of evapotranspiration at spatiotemporal scales (<1000 m and monthly) that can be used to estimate the water balance and the performance of irrigated systems at the canal command scale. This study evaluated the skill of the CMRSET (CSIRO MODIS ReScaled EvapoTranspiration) algorithm to estimate actual evapotranspiration (ET_a) in the 56 canal command areas of the IBIS in Pakistan over the period 2000 to 2018 at 10-day temporal and 500 m spatial resolution. This algorithm was selected as it only requires multi-temporal remote sensing imagery to derive a crop factor and meteorological data for its implementation. To implementation was facilitated by pre-processing satellite reflectance data using the geospatial analysis tool and remote sensing data repository Google Earth Engine. Unlike previous studies of limited duration or spatial domain, these time-series provide the first long-term (>15 years) consistent ET_a time-series for the entire IBIS at spatial and temporal resolutions that are useful to assess irrigation systems at the canal command scale.

To assess CMRSET's accuracy and therefore its usefulness for water balance modelling and other applications, its estimates were evaluated against existing estimates from two remotely sensed ET_a products, SEBAL and ET_{Look} at the pixel and canal command scale, and against ground ET_a measurements at the pixel scale – to assess its accuracy. SEBAL and ET_{Look} were implemented for the year October 2004 to September 2005 and for the calendar year 2007, respectively, and had a comparable spatial and temporal resolution as CMRSET. SEBAL was implemented in the northern part (covering mainly Punjab canal commands) of the study region, and ET_{Look} for the whole Indus Basin (which includes the entire IBIS), therefore the assessment was conducted in 40 canal commands for SEBAL, and 56 canals commands for ET_{Look}. Generally, CMRSET compared well against both datasets, both in terms of magnitude and temporal patterns. CMRSET agreed better to SEBAL in terms of magnitude, with a mean Pearson's correlation coefficient r of 0.85 (min of 0.54 and max of 0.97), a mean absolute percentage bias of 7.6% (min of -12.5% and max of 27.8%), and a mean RMSD of 18.0 mm/mo (min of 9.4 mm/mo and max of 26.7 mm/mo), and no canal command had a bias greater than ±30%. For ET_{Look}, the mean Pearson's correlation coefficient r was 0.93 (min of 0.68 and max of 1.00), the mean absolute percentage bias was 21.4% (min of -23% and max of 77%), and the mean RMSD was 20.5 mm/mo (min of 7.3 mm/mo and max of 49.8 mm/mo). Whilst the temporal patterns were well captured, the resulting magnitudes seemed to be mixed, with 14 canal commands having a percentage bias larger than +30%. CMRSET ET_a estimates were also assessed against two *in situ* Bowen ratio surface energy balance ET_a measurements, that were set up from July 2000 to March 2001 (9 months, during the growing season) in two locations in the Punjab Province. In these locations, CMRSET was also implemented using Landsat (30 m) bands and the same CMRSET model parameters to assess scale differences related to pixel smearing and averaging in the coarser MODIS data (500 m). MODIS CMRSET showed reasonable agreement both in magnitude and seasonality considering the scale differences. For both locations, the Pearson's correlation coefficient r was greater than 0.92, the percentage bias less than 20% and the RMSD less than 17 mm/mo. Results were markedly better for Landsat CMRSET estimates at both locations with bias in both cases being lower than 5%, although with some seasonal compensation reducing bias and RMSD errors.

Considering the differences between CMRSET and the existing remotely sensed products, particular care is required in the use of ET_a for a quantitative water assessment or water balance analyses that uses absolute values, such as the assessment of sustainable groundwater use. Ideally, the results of related applications should be cross-checked for the presence of biases or inconsistencies in relation to the use of this or any other remotely sensed ET_a products. This report is companion to a report that assesses future scenarios

impact on irrigated agriculture using the remotely sensed ET_a products for scenario exploration in a way that the differences do not exert an undue influence in the interpretation of results.

Monthly CMRSET ET_a estimates were used to assess how ET_a changed spatially and temporally in the lower IBIS canal commands during the 2000–2018 period. Temporal resolution was annual (April–March water year) and seasonal – wet Kharif (April to September) and dry Rabi (October to March). The assessment showed that ET_a in most irrigated areas within the canal commands exceeded 600 mm/y, with some areas that exceeded 1000 mm/y, particularly in rice canal commands in the Sindh Rice Wheat agro-climatic zone. Lower mean annual and Kharif ET_a occurred in the Sindh Cotton Wheat South agro-climatic zone and Sindh Rice Wheat South agro-climatic zone canal commands, with around 400 mm to 500 mm (about 100 to 200 mm less) during Kharif. On the other hand, during Rabi, most irrigated areas exceeded 300 mm.

The pre-processing capabilities of Google Earth Engine and continuous update of its satellite imagery catalogue, plus the straightforward implementation of CMRSET ET_a, potentially on a continuous basis, provides an opportunity for monitoring irrigation dynamics and the assessment of structural and policy improvements in the IBIS.

1 Introduction

The Indus Basin Irrigation System (IBIS) provides food and economic security for about 207 million people in Pakistan. The semi-arid climate and nearly-fully allocated surface and groundwater water resources represent a continuous management challenge. The construction and improvement of hydraulic infrastructure that regulates and conveys available water has played a pivotal role to increase the efficiency of existing irrigation systems. Diagnosing the improvements in irrigation performance by implementing such dedicated infrastructure has been hampered by lack of enough water supply and use data. Satellite Remote Sensing (RS) may be the only means to provide robust and consistent estimates in large irrigated areas and associated water use at a policy relevant scale (i.e. canal commands or <1 km spatial scale and monthly temporal resolution). Multi-temporal RS data can potentially provide crop types, extent and associated actual crop evapotranspiration (ET_a), which can then be used to assess irrigation dynamics and performance in large irrigation systems such as the IBIS, and to inform and improve water management (Ahmad et al., 2009).

The purpose of this report is to present the results of the implementation and evaluation of a RS ET_a algorithm in the IBIS, the CMRSET (CSIRO MODIS ReScaled EvapoTranspiration, Guerschman et al., 2009) algorithm, followed by a spatial and temporal analysis of the ET_a dynamics in canal commands in the Sindh Province. The implementation spans 2000 to 2018 at 10-day temporal and 500 m spatial resolution, making it the first long-term time-series (>15 years) for the IBIS at spatial and temporal resolutions that are useful to assess irrigation systems at the canal command scale. Previous estimates of ET_a in the IBIS were performed for a single year or a limited number of years, for a constrained spatial domain (e.g. Ahmad et al., 2008, 2009; Bastiaanssen et al., 2012).

CMRSET estimates were evaluated to assess their accuracy and therefore their usefulness for water balance modelling and other applications. CMRSET was evaluated against (i) other previously implemented RS ET_a algorithms – SEBAL (Ahmad et al., 2008) and ET_{Look} (Bastiaanssen et al., 2012; Cheema, 2012) - at the pixel and canal command scale and (ii) *in situ* Bowen ratio ET_a measurements at the pixel scale (Ahmad et al., 2002).

This report is a companion to the report on assessments of climate change and dam sedimentation impacts and urban water supply on irrigated agriculture in the Punjab and Sindh provinces (Ahmad et al., 2020a and Ahmad et al. 2020b). The results described here are used as one of the inputs for the exploratory future scenarios described in Ahmad et al. (2020a; 2020b).

Following this introduction, the remainder of this report is as follows: Section 2 presents the study region, methods and materials follow in Section 3, Section 4 presents results followed by summary and conclusion in Section 5.

2 Study region

The study region overlays the IBIS (~140,000 km^2,) within the Indus Basin (1,125,000 km^2). The IBIS is the largest contiguous irrigation system in the world (Condon et al., 2014). The region, located south of the Himalayan mountains, is comprised of mostly flat topography with rich soils resulting from the erosion of the Himalayan mountains and deposition in large alluvial valleys. The region's climate is influenced by the South Asian Monsoon, with most of the annual precipitation occurring from June to September. The monsoon is the annual reversal of wind direction caused by excess heating over the South Asian land mass. It draws moisture from the Arabian Sea and Bay of Bengal into South Asia, across Pakistan and into the southern upper Indus Basin (where most precipitation occurs) during June to September (Charles et al., 2016). Precipitation has a strong northeast-to-southwest gradient, with about 1800 mm per year precipitating in the Himalayas to about 200 mm per year in the south of the IBIS (Hutchinson and Xu, 2013, Stewart et al., 2018).

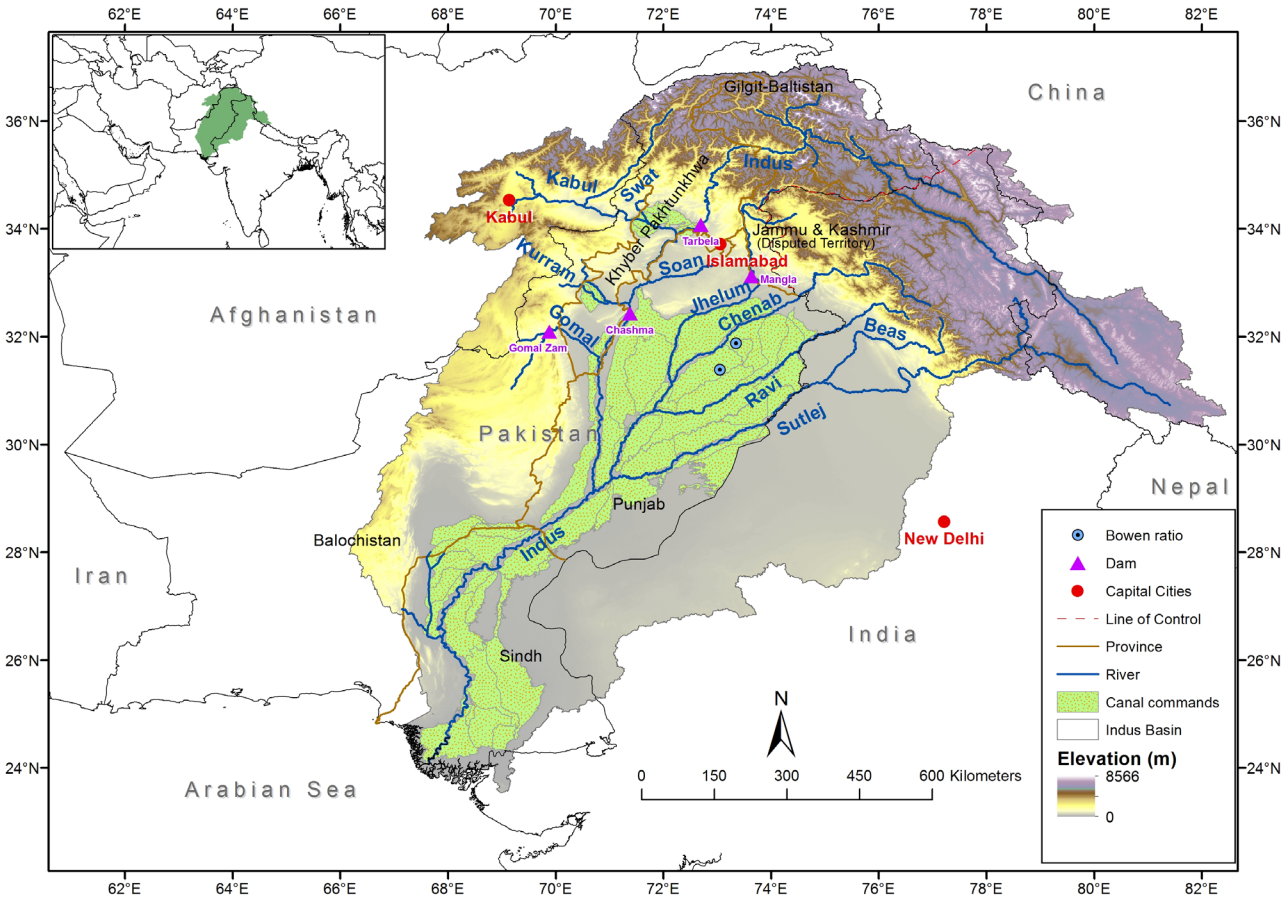

Figure 2-1 Geographic characteristics of the Indus Basin Irrigation System including main rivers, canal commands and location of two Bowen ratio stations

The main rivers supplying the IBIS are the Chenab, Jhelum, Indus and Kabul, whereas the Sutlej and Ravi have most of their flows diverted in India before entering Pakistan (Figure 2-1). Within Pakistan, approximately 75% (131 km^3) of the mean annual flow in the Indus river (175 km^3) is diverted to agriculture (mainly in the IBIS) producing 90% of the food for Pakistan (Stewart et al., 2018).

There are 60 main canal commands areas (existing, plus those that are planned or under construction) along the main rivers in the IBIS (numbered from north to south, Figure 2-2.). Irrigated agriculture accounts for

about 85 % of cereal production, all sugar production and nearly all cotton production (Archer et al., 2011). Surface water is diverted from a river's main course through an extensive network of barrages and canals to canal commands so it can be used for irrigation for a wide range (50+) crops and horticulture through the growing season. Horticulture and sugarcane are annual crops. The dominant Kharif (April to September) crops are cotton, rice, maize and fodder. Wheat and fodder are the dominant crops during the Rabi (October to March) season (Kirby et al., 2017, Ahmad et al., 2019).

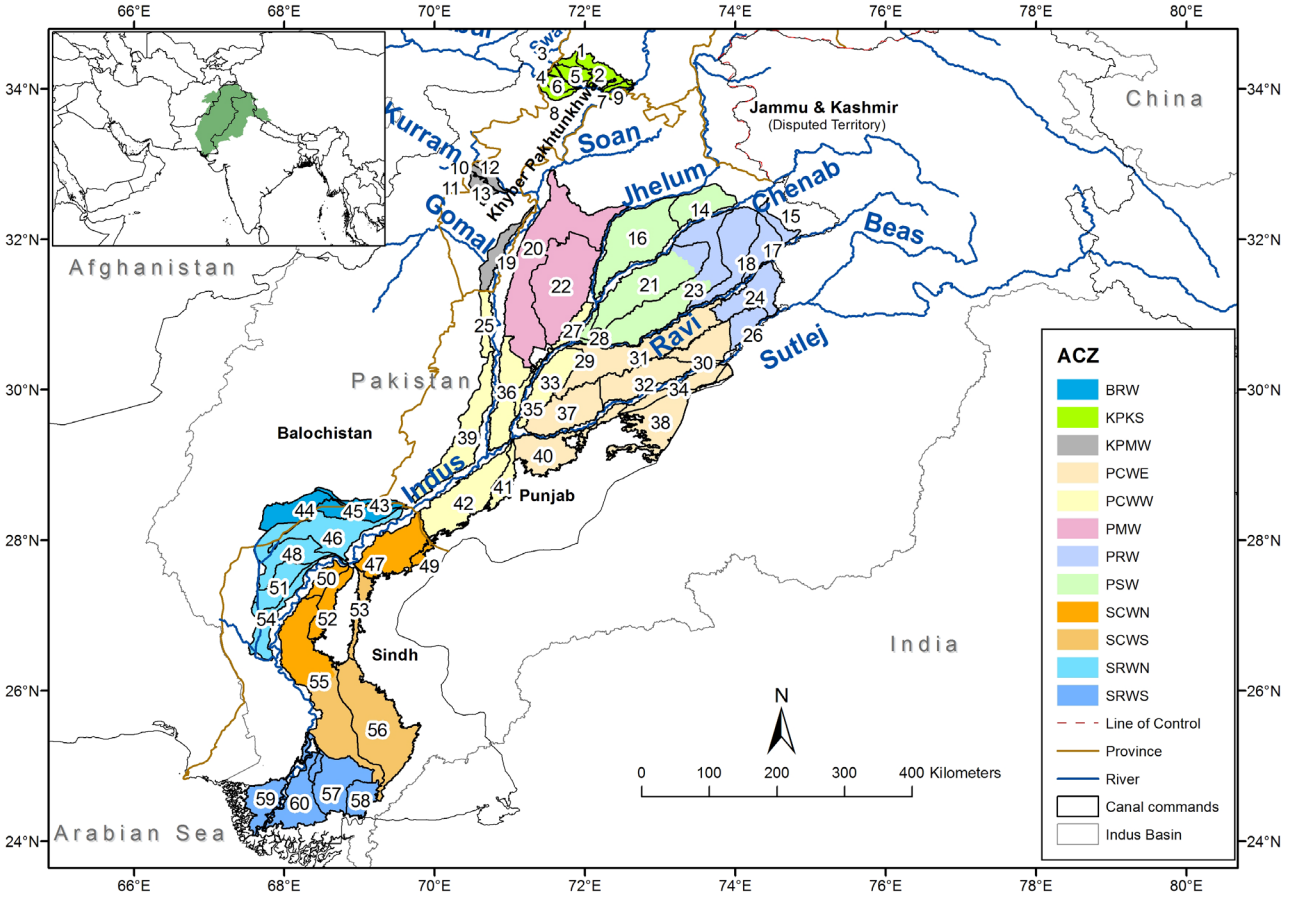

Figure 2-2 Canal commands and the corresponding agro-climatic zones (ACZ) in the IBIS. Canal commands are labelled from north to south.Source: Indus River System Authority (IRSA). A summary of canal commands and identification number can be found in Appendix A. BRW=Balochistan Rice Wheat, KPKS=Khyber Pakhtunkhwa Sugarcane, KPMW= Khyber Pakhtunkhwa Mixed Crops West, PCWE=Punjab Cotton Wheat East, PCWW=Punjab Cotton Wheat West, PMW=Punjab Mixed Crops West, PRW=Punjab Rice West, PSW=Punjab Sugarcane West, SCWN=Sindh Cotton Wheat North, SCWS= Sindh Cotton Wheat South, SRWN=Sindh Rice Wheat North, SRWN=Sindh Rice Wheat South

In this report, provinces and crop types define 12 different Agro-Climatic Zones (ACZ) for the canal commands (Figure 2-2). Punjab and Sindh Provinces are the main irrigated areas, and cotton and/or rice (Kharif) and wheat (Rabi) are the main crops. For example, PRW corresponds to Punjab Rice Wheat, whereas PCWW corresponds to Punjab Cotton Wheat West, PMW corresponds to Punjab Mixed Wheat and PSW corresponds to Punjab Sugarcane West. Accordingly, SCWN corresponds to Sindh Cotton Wheat North, and so on. Other provinces included are Balochistan (B) and Khyber Pakhtunkhwa (KP), which follow the same rationale as explained above. A summary of canal commands and their identification numbers (as in Figure 2-2) can be found in Appendix A .

3 Methods and materials

3.1 Long-term 10-day CMRSET ET_a time-series estimates

The CMRSET (CSIRO MODIS ReScaled EvapoTranspiration, Guerschman et al., 2009) algorithm was used to estimate ET_a at a temporal resolution of 10 days and spatial resolution of 500 m for the 2000–2018 period. Monthly ET_a is estimated by scaling Hargreaves potential evapotranspiration (ET_p) via a remote sensing-based crop factor (K_c), which is obtained from two indices – the Enhanced Vegetation Index (EVI, Huete et al., 2002) and the Global Vegetation Moisture Index (GVMI, Ceccato et al., 2002). EVI and GVMI can be used to discriminate open water when EVI is low and GVMI is high, and to detect vegetation water content when EVI is high. The main advantages of CMRSET are that it uses a single set of parameters (i.e. does not need an auxiliary land cover map) and it does not require manual calibration to detect wet or dry pixels, as in some energy balance algorithms. Also, CMRSET can estimate ET_a in areas with significant direct evaporation, including lakes and floodplains. CMRSET has been evaluated in several studies, in different climates and for different applications, including: water assessment modelling (Paca et al., 2019; Peña-Arancibia et al., 2016, 2019; van Dijk et al., 2011), ecosystem mapping (Barron et al., 2014; Peña-Arancibia et al., 2014) and recharge studies (Crosbie et al., 2014; Silberstein et al., 2013). Three steps are required to obtain time-series of 500 m, 10-day K_c, ET_p and ET_a, respectively:

1) 10-day EVI and GVMI composites at 500 m spatial resolution for the entire IBIS were obtained via Google Earth Engine (Gorelick et al., 2017) from the daily Moderate Resolution Imaging Spectroradiometer (MODIS) surface spectral reflectance product (MOD09GA, collection 6). The average pixel value was selected within the 10-day composite, while minimising cloud cover and nulls. The 10-day EVI and GVMI were extracted from February 2000 to December 2018. Any gaps prevailing in the vegetation indices time-series were filled using Harmonic ANalysis of Time Series (HANTS, Zhou et al., 2015).

2) Daily gridded surfaces (2.5 km resolution, Hutchinson and Xu, 2013) minimum and maximum temperature were used to calculate ET_p following Hargreaves (1974) for the 2000–2013 period. To update the daily ET_p until 2018, daily Hargreaves ET_p (250 km resolution) was computed via Google Earth Engine from the Global Land Data Assimilation System (GLDAS) Version 2.1 (Rodell et al., 2004). Further, both gridded datasets were accumulated to 10-day to match the temporal resolution of the EVI and GVMI VIs for further upscaling. Finally, the GLDAS ET_p were oversampled to 2.5 km spatial resolution, and bias-corrected and evaluated for consistency using 10-day scaling factors obtained from the 2000–2013 period, in which both gridded ET_p datasets overlapped.

3) 10-day ET_a for 2000–2018 was estimated with the following procedure: First, a residual Moisture Index (RMI) was developed by combining EVI and GVMI. EVI and GVMI respond positively to increases in near-infrared reflectance, therefore the two indices have a relatively high correlation (Guerschman et al., 2009). If the correlation between the two indices is removed, the residuals could be used as an indicator of vegetation moisture (Guerschman et al., 2009). The Residual Moisture Index (RMI) was calculated for each pixel as the vertical distance between its corresponding GVMI and a baseline as follows:

   $$RMI=\max(0, GVMI-(K_{RMI}\times EVI+C_{RMI}), \quad \text{Eq. 1}$$

   where C_{RMI} and K_{RMI} are calibrated parameters which describe the exact position of the baseline, in this way most of the correlation between the two indices was eliminated. The exact position of the baseline was calculated using MODIS EVI and GVMI data for all the pixels in Australia for the months

of January, May and September 2001. These are considered representative for this study region, given the range of EVI-GVMI combinations represented in Australia and similar climatic characteristics corresponding to semi-arid areas. The values for K_{RMI} and C_{RMI}, after calibration, were 1.778 and -0.350, respectively.

4) Secondly, K_c was estimated as follows:

$$K_c=K_{c\_max}\times(1-\exp(-a\times EVI^{\alpha}-b\times RMI^{\beta}), \quad \text{Eq. 2}$$

where K_{c_max} is multiplied by a sigmoidal function of EVI and RMI. The model was calibrated for MODIS data using eddy-covariance ET_a from seven flux towers in Australia and validated with water balance data for 227 unimpaired catchments across Australia (Guerschman et al., 2009). The parameters used herein had the following values: K_{c_max}=1.00, a=14.42, α=2.701, b=2.086, β=0.953. Finally, ET_a was obtained by scaling ET_p with the estimated K_c as:

$$ET_a= K_c\times ET_p. \quad \text{Eq. 3}$$

3.2 Comparison of CMRSET ET_a against SEBAL and ET_{Look}

CMRSET ET_a was compared against two remote sensing ET_a datasets previously implemented in the study region (or part thereof): ET_{Look} (Bastiaanssen et al., 2012; Cheema, 2012) and SEBAL (Ahmad et al., 2008).

ET_{Look} uses soil moisture derived from passive microwave sensors as the driving force for calculation of a surface energy balance that includes a soil moisture component. The advantage of this method is that is not hampered by cloud cover and it allows estimation of ET_a at finer than 10-day temporal resolution. ET_{Look} uses simple downscaling methods to oversample the 25 km spatial resolution passive microwave data from the Advanced Microwave Scanning Radiometer (AMSR-E) on the Aqua satellite to 1 km spatial resolution. ET_{Look} requires ancillary data (other than soil moisture) common to other radiation and energy balance methods: spectral vegetation index, surface albedo, atmospheric optical depth, land use and land cover data, soil physical properties, and meteorological data. Bastiaanssen et al. (2012) estimated 8-day ET_a using the ET_{Look} method for the entire Indus Basin for the calendar year 2007.

SEBAL is a well-tested algorithm and has been evaluated in several countries against *in situ* data (see Ahmad et al., 2009 and references therein). SEBAL resolves the radiation and energy balance, it requires manual calibration to pick dry and wet pixels used to estimate the sensible heat flux of the energy balance. The dry and wet pixels are manually selected, based on vegetation index, surface temperature, albedo and some basic knowledge of the study area (Ahmad et al., 2009). Ahmad et al. (2008) implemented the monthly SEBAL algorithm using MODIS (MOD021KM, collection 5) calibrated Radiances at 1 km spatial resolution for the year 2004–2005 (October to September) for the Punjab province, which corresponds to the northern parts of the IBIS.

Both RS ET_a datasets (ET_{Look} and SEBAL) were oversampled to 500 m resolution for comparison with CMRSET. The evaluation was performed for 56 (or 40 for SEBAL) out of the 60 canal command areas provided by the Indus River System Authority (IRSA). Four canal commands were excluded because they were under construction or planned for construction in the future or did not have any discernible irrigated areas during the comparison time period. The presence/absence of irrigation was assessed by estimating mean 10-day maximum and minimum EVI values aggregated at the canal command and further verified using Google Earth.

Temporal and spatial comparisons between CMRSET and the two RS datasets were conducted:

- For the temporal comparison, canal command monthly aggregated time-series ET_a values for the corresponding years were compared visually and the following goodness-of-fit-statistics were computed: Pearson's correlation coefficient (r), percentage bias and root mean square difference (RMSD).

- For the spatial comparison, canal command pixels for all months for the corresponding years were compared one-to-one visually and the following goodness-of-fit- statistics were computed: Pearson's correlation coefficient (r), percentage bias and root mean square difference (RMSD).

3.3 Comparison of CMRSET ET_a against two locations with Bowen ratio ET_a estimates

Bowen ratio surface energy balance measurement systems to directly measure ET_a were set up in a cotton-wheat field (co-ordinates: 73°2′49.8′′E, 31°23′26.2′′N) at Faisalabad and a rice-wheat field (co-ordinates: 73°20′50.2′′E, 31°52′34.2′′N) at Pindi Bhattian in 2000 (Ahmad 2002, Ahmad et al., 2002). Bowen ET_a measurements were aggregated to monthly for comparison with CMRSET and were available from July 2000 to March 2001. The following goodness-of-fit-statistics were computed: Pearson's correlation coefficient, percentage bias and root mean square difference (RMSD).

3.4 ET_a spatial and temporal dynamics for the IBIS and for canal commands

The ET_a monthly time-series were used to assess the similarities and differences between canal commands and associated ACZs. The ET_a dynamics assessment was conducted both spatially and temporally for the lower IBIS canal commands, located in the Sindh Province (Balochistan canal commands were also included for completeness, as the streamflow that enters the irrigation systems are shared for the 2000–2018 period), including:

- Description of ET_a spatial annual mean maps for a hydrological year (April to March for the 2000–2018 period), and seasonal mean maps for the wet (Kharif, April to September) and dry (Rabi, October to March) seasons, highlighting differences between ACZs.
- Description of seasonal time-series for canal commands, aggregated by canal deliveries surface water source.

4 Results and discussion

4.1 Long-term 10-day CMRSET ET_a time-series estimates

CMRSET ET_a was estimated at 10-day temporal resolution and 500 m spatial resolution for the 2000–2018 period. The two ET_p datasets used were: (i) the 10-day Hargreaves ET_p obtained from daily gridded surfaces (2.5 km resolution) minimum and maximum temperature for the 2000–2013 period and, (ii) 10-day Hargreaves ET_p (250 km resolution) from the Global Land Data Assimilation System (GLDAS) Version 2.1. The GLDAS ET_p were oversampled to 2.5 km spatial resolution, and bias-corrected using: (i) 10-day scaling factors obtained from the period 2000–2013 and (ii) using cumulative distribution function (CDF) matching for each grid cell (Reichle and Koster, 2004; Yin and Zhan, 2018) for the overlapping period, and evaluated for consistency. Both resulting monthly CMRSET ET_a time-series for the year 2013 aggregated to the canal command scale were compared in the 56 canal commands (Figure 4-1).

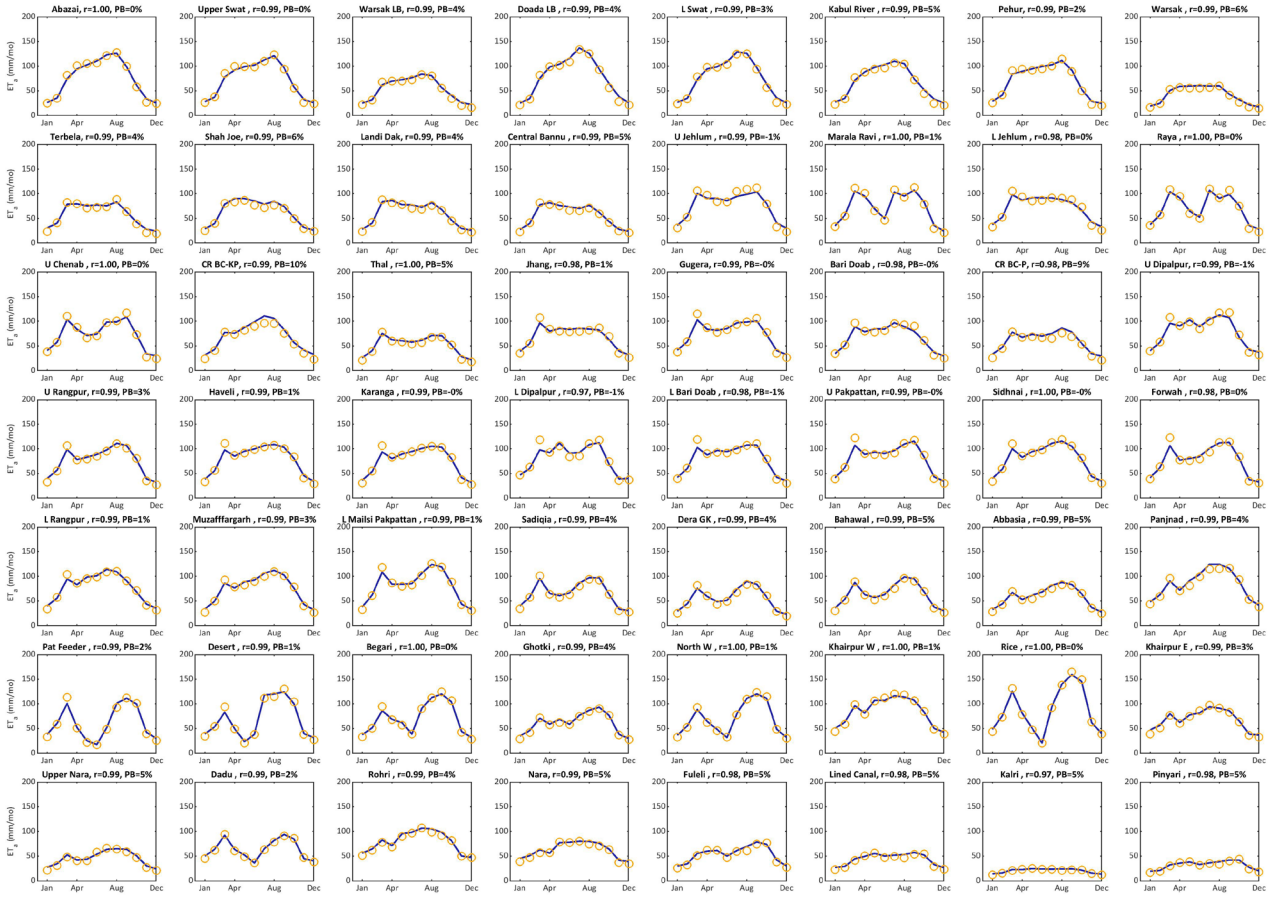

Figure 4-1 Comparison of monthly CMRSET ET_a time-series for the year 2013 aggregated to the canal command scale for 56 canal commands. CMRSET using daily gridded 2.5 km ET_p surfaces (blue lines) and CMRSET using rescaled GLDAS ET_p (red circles). Canal commands are reported from north to south across rows from left to right

It is readily apparent that both datasets are very similar both in terms of magnitude and temporal patterns. The mean Pearson's correlation coefficient r is 0.99, mean absolute percentage bias is 2.7%, and the RMSD is 4.4 mm/mo.

The pixel by pixel comparison for all months for 2013 were compared one-to-one in the 56 canal commands with results showing no major differences in either dataset (Figure 4-2).

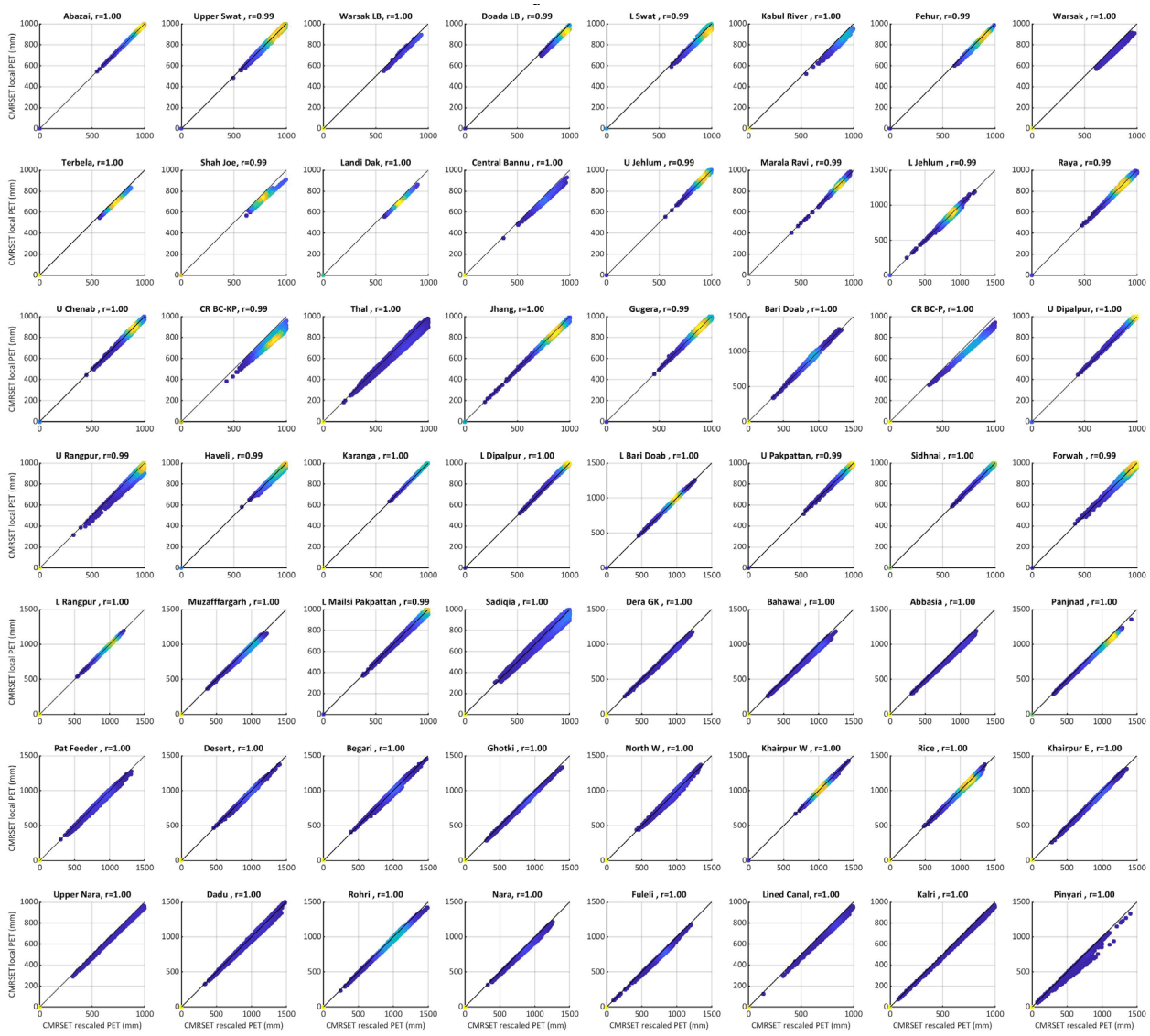

Figure 4-2 Density plot of the pixel by pixel comparison for 56 canal commands. Canal commands are reported from north to south across rows from left to right. The colour ramp shows the data density, with blue through yellow to red denoting lower to higher density. Note that the maximum and minimum values to determine the ramp are per panel

Figure 4-3 shows the mean hydrologic year (April to March) spatial distribution of ET_a in the IBIS canal commands. The mean ET_a for the 2000–2018 period is 485 mm/y, with a minimum ET_a of 404 and maximum of 530 mm/y, in 2002 and 2013 respectively. There is large spatial variability within canal commands due to the presence of arid and intensively cropped areas, with mean minimum ET_a of 35 mm/y and mean maximum ET_a of 1938 mm/y. ET_a remains within 20% of the mean in each hydrologic year, controlled by relatively stable areas of high ET_a in canal commands.

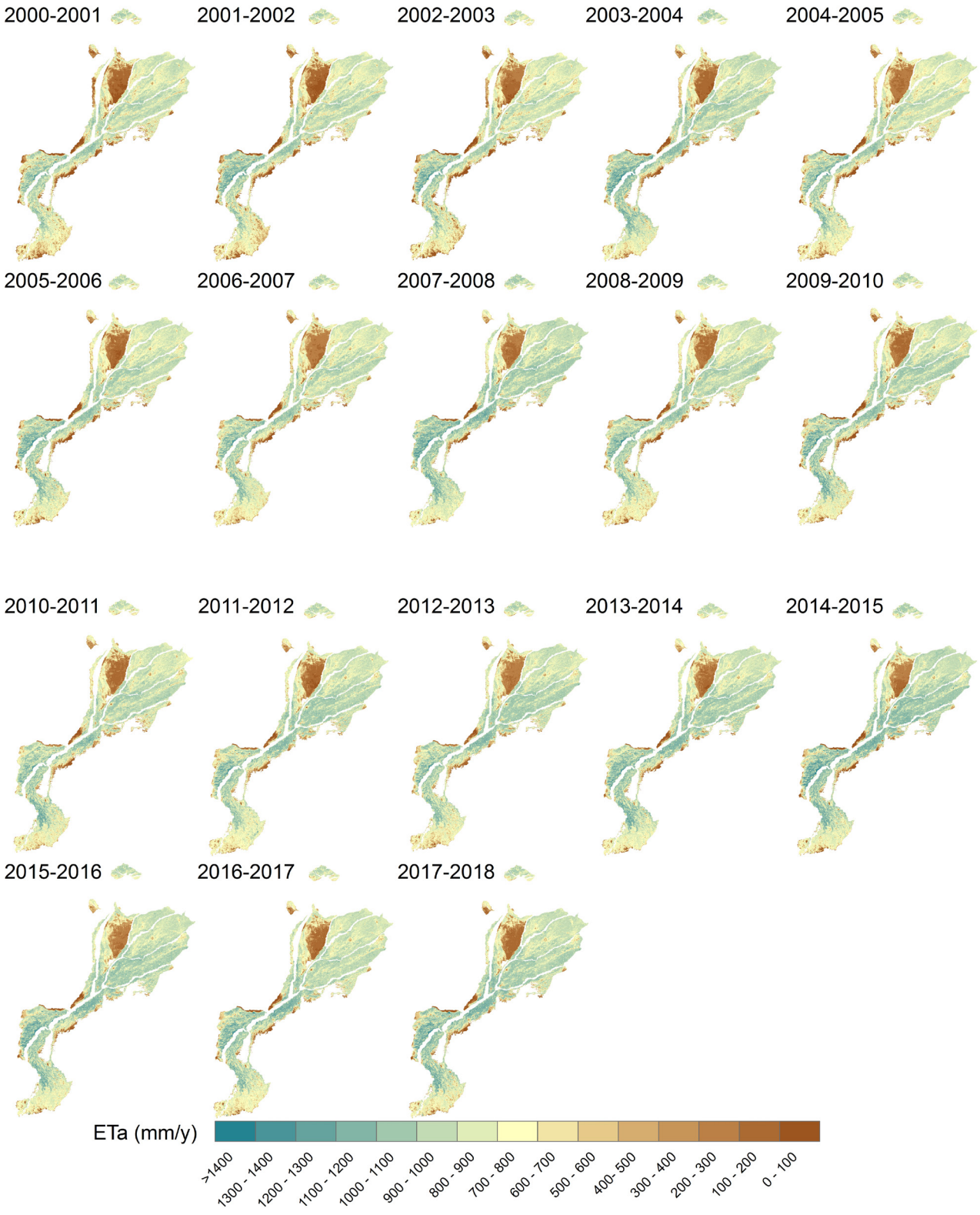

Figure 4-3 Spatial ET_a time-series for each hydrologic year (April to March) from 2000–2001 to 2017–2018

4.2 Comparison of CMRSET ET_a against two RS products

4.2.1 Comparison of CMRSET ET_a against ET_{Look}

Figure 4-4 shows the comparison of monthly CMRSET and ET_{Look} ET_a time-series for the calendar year 2007 aggregated to the canal command scale for 56 canal commands. The results described herein are tabulated in Appendix A.1. Both datasets agree reasonably well both in terms of magnitude and temporal patterns. The mean Pearson's correlation coefficient r is 0.93 (min of 0.68 and max of 1.00), the mean absolute percentage bias is 21.4% (min of -23% and max of 77%), and the mean RMSD is 20.5 mm/mo (min of 7.3 mm/mo and max of 49.8 mm/mo). Whilst the temporal patterns are well captured as shown in Figure 4-4, the resulting magnitudes seem to be mixed, with CMRSET being higher in some areas and lower in some others. CMRSET is higher than ET_{Look} in the canal commands in KPKS and KPMW (Figure 2-2) during most months, with a mean bias of 29.6%. CMRSET is somewhat higher or slightly lower with a bias generally lower than 25% in the canal commands north-east of the Indus River, including canal commands in PSW, PRW and PCWE (except for Sadiqia, Bahawal and Forwah). In canal commands in PCWW (except for Sidnhai, east of the Indus River), CMRSET is higher, more so in the canal commands that have large non-vegetated areas (see EVI time-series in Figure 4-4) with a mean bias of 26.9%. CMRSET is lower than ET_{Look} in canal commands in BRW (mean bias of -10,7%) and in canal commands in SRWN the mean bias is -11.5%. Results are mixed in canal commands in SCWN, with CMRSET being in close agreement with ET_{Look} in Khairpur West (bias of 10.7%) and Rohri (bias of 10.5%), but higher for Khairpur East (bias of 39.4%) and Ghotki (bias of 27.3%). CMRSET is in close agreement with ET_{Look} in the canal commands in SRWN and SRWS, with most canals having a bias lower than 20%, except for Kalri (SRWS, bias of 28.5%) and North W (bias of -23.8). CMRSET is higher in canal commands in SCWS with a mean bias of 54%, note that Upper Nara has a bias of 77% and Nara of 32%.

Figure 4-5 shows density scatterplots of monthly pixel by pixel CMRSET and ET_{Look} ET_a for the calendar year 2007 for 56 canal commands. These plots can be used to interpret both the agreement between pixels of CMRSET and the RS ET_a products. A perfect agreement would show all pixels sitting on the 1:1 line. The density colour map – from blue (less dense) to yellow (denser) – shows the distribution of ET_a within the canal command. Overall, CMRSET and ET_{Look} compare well, the mean Pearson's correlation coefficient r is 0.74 (min of -0.05 and max of 0.98). For the canal commands in KPKS, the mean r is 0.55 (min of -0.05 and max of 0.94) and the density plots show that CMRSET is generally higher than ET_{Look}, with most pixels falling to the right of the 1:1 line, except for Upper Swat and Kabul River. For the canal commands in KPMW, the mean r is 0.78 (min of 0.74 and max of 0.83) and the density plots show that CMRSET is higher than ET_{Look}, with most pixels falling to the right of the 1:1 line. For the canal commands in PSW, the mean r is 0.82 (min of 0.70 and max of 0.95) and the density plots show that CMRSET agrees well with ET_{Look}, with most pixels falling around the 1:1 line. For the canal commands in PRW, the mean r is 0.46 (min of 0.03 and max of 0.71) and the density plots show that CMRSET agrees well with ET_{Look}, with most pixels falling around the 1:1 line, except for Raya and Marala Ravi, where CMRSET is higher than ET_{Look} (note that the low r value in Marala Ravi seems to be an statistical artefact due to the high concentration of pixels in one location). For the canal commands in PCWW, the mean r is 0.82 (min of 0.70 and max of 0.89) and the density plots show that CMRSET is higher than ET_{Look}, with most pixels falling to the right of the 1:1 line, except for Panjad that is more in agreement. For the canal commands in PCWE, the mean r is 0.73 (min of 0.53 and max of 0.86) and the density plots show that CMRSET agrees well with ET_{Look}, with most pixels falling around the 1:1 line, except for Sadiqia and Bahawal, where CMRSET is higher than ET_{Look}. For the canal commands in BRW and SRW, the mean r is 0.92 (min of 0.89 and max of 0.98) and the density plots show that CMRSET agrees well with ET_{Look}, with most pixels falling around the 1:1 line, although CMRSET shows less variability than ET_{Look}. For the canal commands in SCWN, SCWS and SRWS, the mean r is 0.84 (min of 0.65 and max of 0.98) and the density plots show that CMRSET agrees well with ET_{Look}, with most pixels falling around the 1:1 line, except for Khairpur E and Upper Nara (both SCWN canals), where CMRSET is higher than ET_{Look}.

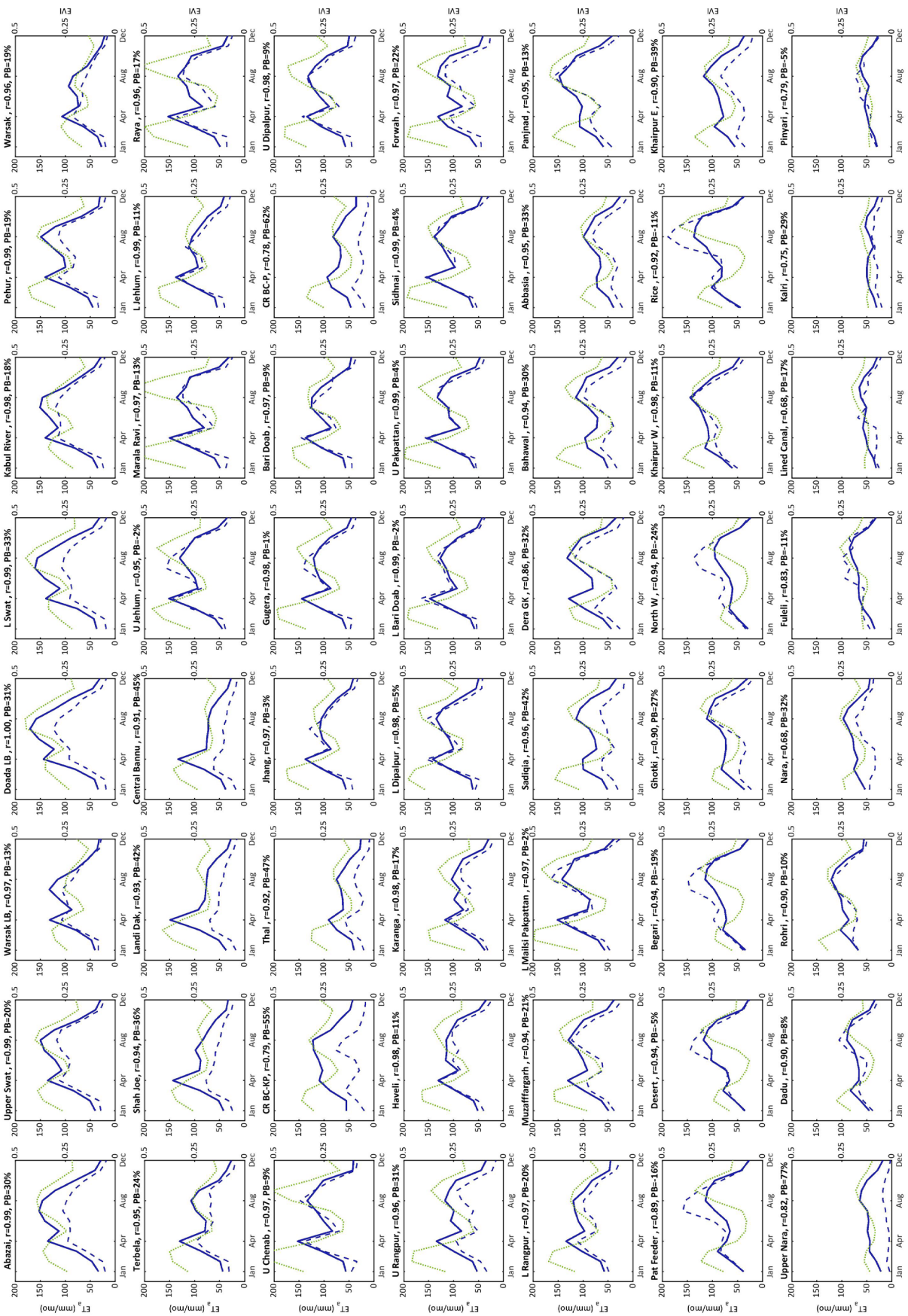

Figure 4-4 Comparison of monthly CMRSET (solid blue line) and ET_{Look} (dashed blue line) ET_a time-series for the calendar year 2007 aggregated to the canal command scale for 56 canal commands. The Enhanced Vegetation Index (EVI) aggregated time-series is shown for reference (green line). Canal commands are reported from north to south across rows from left to right

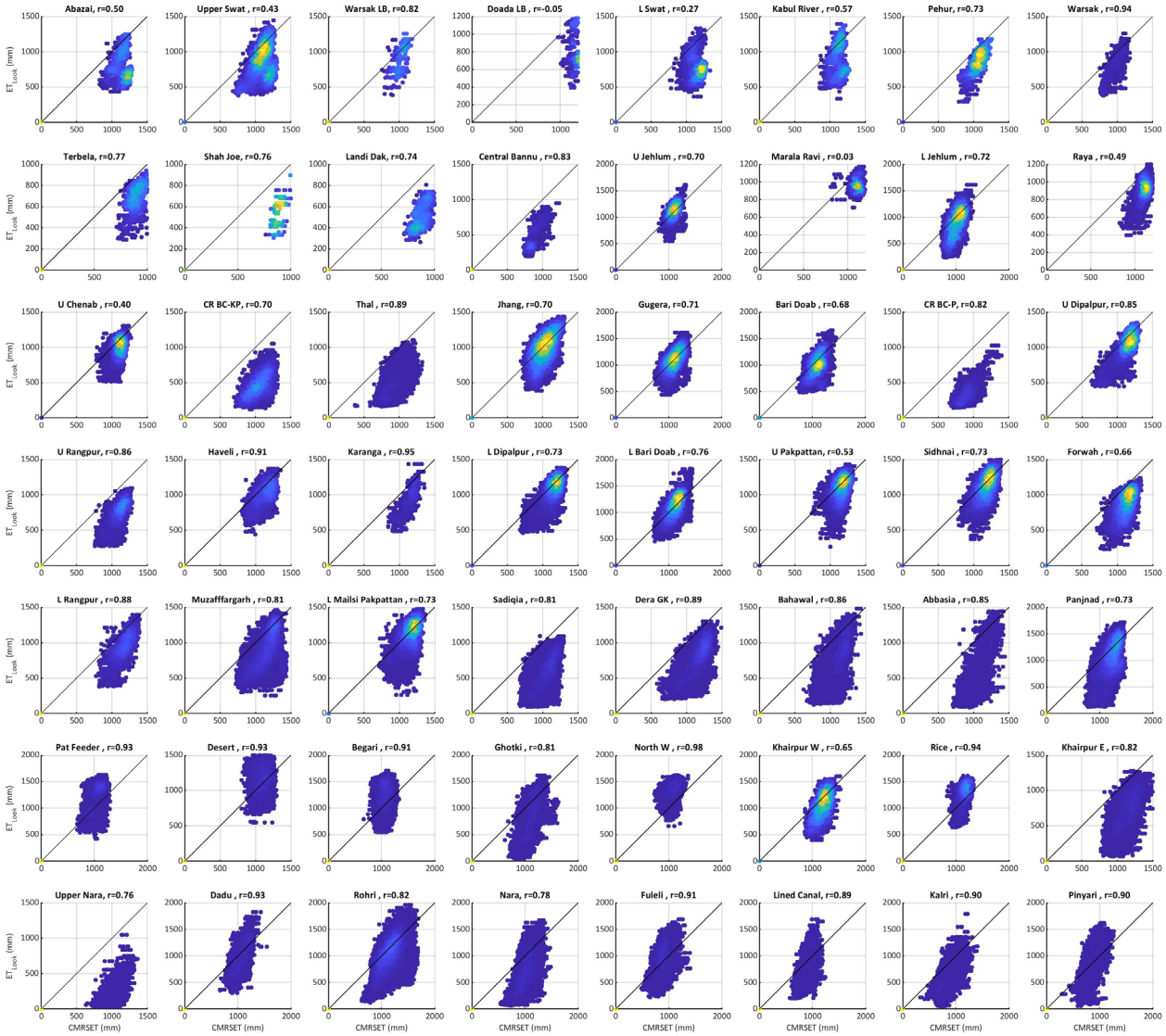

Figure 4-5 Density scatterplots of monthly pixel by pixel CMRSET (X-axis) and ET_{Look} (Y-axis) ET_a for the calendar year 2007 and for 56 canal commands. Canal commands are reported from north to south across rows from left to right. The colour ramp shows the data density, with blue through yellow to red denoting lower to higher density. Note that the maximum and minimum values to determine the ramp are per panel

4.2.2 Comparison of CMRSET ET_a against SEBAL

Figure 4-6 shows the comparison of monthly CMRSET and SEBAL ET_a time-series for the year 2004–2005 aggregated to the canal command scale for 40 canal commands. Both datasets agree reasonably well both in terms of magnitude and temporal patterns. The mean Pearson's correlation coefficient r is 0.85 (min of 0.54 and max of 0.97), the mean absolute percentage bias is 7.6% (min of -12.5% and max of 27.8%), and the mean RMSD is 18.0 mm/mo (min of 9.4 mm/mo and max of 26.7 mm/mo). Both the temporal patterns and magnitudes compare well as shown in Figure 4-6. CMRSET agrees well with SEBAL in most canal commands, although June-July ET_a peaks are lower in CMRSET than in SEBAL for Marala Ravi, Raya and Upper Chenab (PRW), and Lower Dipalpur (PCWE). Figure 4-7 shows density scatterplots of monthly pixel by pixel CMRSET and SEBAL ET_a for the year 2004–2005 aggregated to the canal command scale for 40 canal commands. Overall, CMRSET and SEBAL compare well, the mean Pearson's correlation coefficient r is 0.58 (min of -0.25 and max of 0.94). The density plots show that CMRSET agrees well with SEBAL, with most pixels falling around the 1:1 line, except for Bahawal, Abbasia and Panjad where the density plots show that CMRSET is higher than SEBAL, with most pixels falling to the right of the 1:1 line.

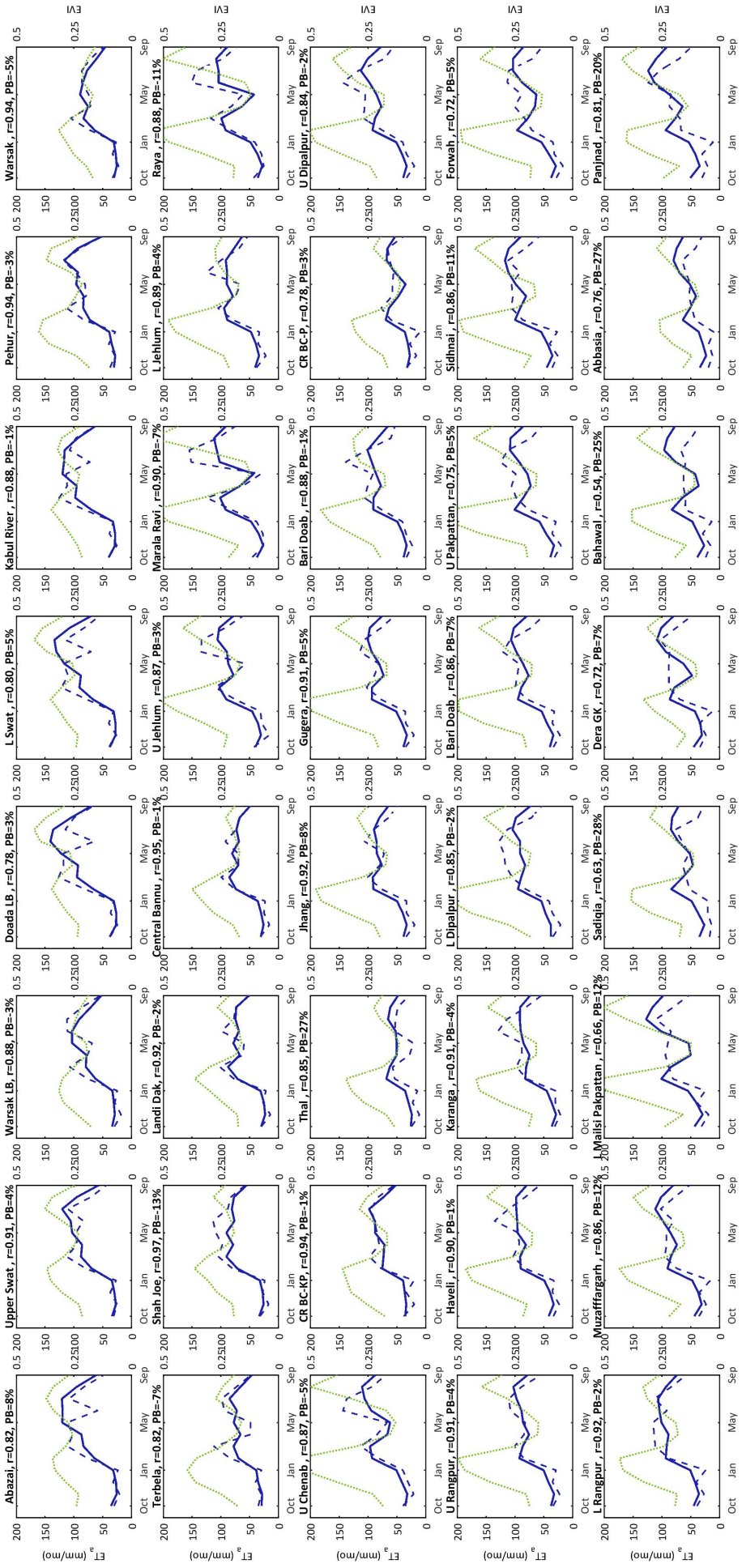

Figure 4-6 Comparison of monthly CMRSET (solid blue line) and SEBAL (dashed blue line) ET_a time-series for the year 2004–2005 (October to September) aggregated to the canal command scale for 40 canal commands. The Enhanced Vegetation Index (EVI) aggregated time-series is show for reference (green line). Canal commands are reported from north to south across rows from left to right

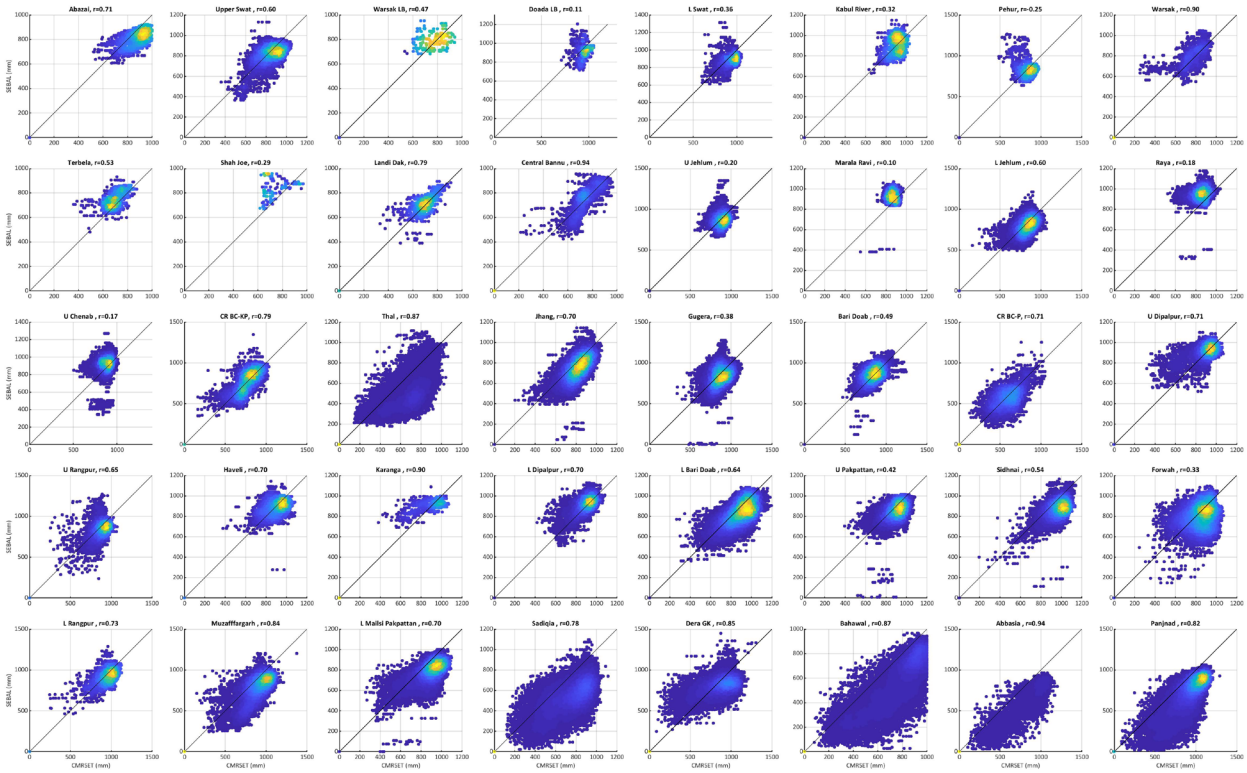

Figure 4-7 Density scatterplots of monthly pixel by pixel CMRSET (X-axis) and SEBAL (Y-axis) ET_a for year 2004–2005 (October to September) aggregated to the canal command scale for 40 canal commands. Canal commands are reported from north to south across rows from left to right. The colour ramp shows the data density, with blue through yellow to red denoting lower to higher density. Note that the maximum and minimum values to determine the ramp are per panel

4.2.3 Differences between the ET_a products

The comparison between CMRSET ET_a against SEBAL and ET_{Look} at the pixel and canal command scale showed that although temporal patterns are largely similar, there are differences in magnitudes. This is somewhat expected given the differences in the models, from a somewhat simple vegetation index approach in CMRSET, increasing complexity in the land surface temperature (LST) approach in SEBAL, to the combined passive microwave-LST approach in ET_{Look} further constraining soil moisture availability. The time series density scatterplots, particularly in the canal commands in the southern IBIS (see Figure 2-2 and comparisons between CMRSET and ET_{Look} in these canals), show that CMRSET tends to overestimate ET_a in dry pixels/areas when compared to ET_{Look}. Conversely, this overestimation does not seem to occur when CMRSET ET_a is compared to SEBAL. Some irrigation landscapes that are highly spatially heterogenous at the 500 m pixel scale (for example narrow irrigated strips along the Upper Nara Canal) may present a challenge for ET_{Look} which relies on downscaled 25 km spatial resolution passive microwave data. This may be more pronounced at the interface between irrigated and non-irrigated areas. On the other hand, some overestimation in CMRSET may be related to CMRSET's lack of mechanism to induce stomatal closure when there is strong stress associated to temperature or water availability. Again, the agreement in the time series (particularly in canal commands intensively irrigated) and density scatterplots suggest this is not expected to be an issue in wetter and irrigated areas.

4.3 Comparison of CMRSET ET_a against two locations with Bowen ratio ET_a estimates

Bowen ratio surface energy balance ET_a measurements were set up from July 2000 to March 2001 in two locations in the Punjab Province (Figure 4-8), one in a cotton field at Faisalabad and the other in a rice paddy at Pindi Bhattian. Monthly CMRSET ET_a for both MODIS (500 m spatial resolution) and Landsat (30 m spatial resolution, USGS Landsat 5 Surface Reflectance Tier 1) were compared to monthly ET_a Bowen ratio measurements. Landsat data were used to asses scale differences related to pixel smearing and averaging in the coarser MODIS data. MODIS CMRSET shows reasonable agreement both in magnitude and seasonality considering the scale differences (Figure 4-8). In Faisalabad, the Pearson's correlation coefficient r is 0.95, the percentage bias is 16.3%, and the mean RMSD is 17.0 mm/mo. In Pindi Bhattian, the Pearson's correlation coefficient r is 0.92, the percentage bias is -3.9%, and the mean RMSD is 16.4mm/mo. As expected, results were better for Landsat CMRSET estimates at both locations with bias in both cases being lower than 5%.

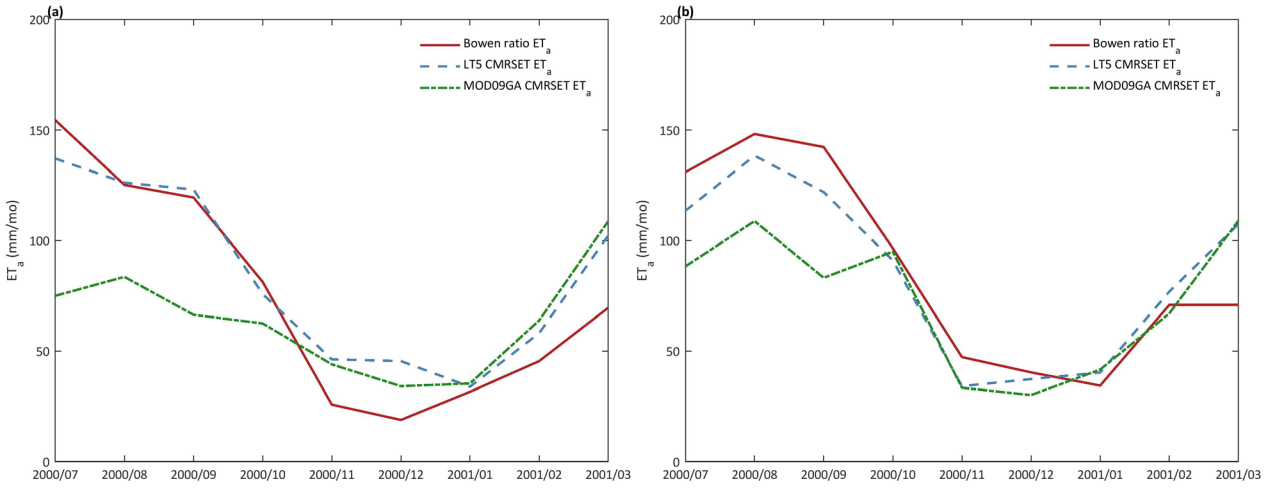

Figure 4-8 Comparison between monthly CMRSET ET_a for both MODIS (500 m spatial resolution green dashed line) and Landsat (30 m spatial resolution, blue dashed line) and ET_a from Bowen ratio measurements at two locations in Punjab: (a) cotton filed at Faisalabad and (b) rice paddy at Pindi Bhattian

4.4 ET_a spatial and temporal dynamics in the lower IBIS

The ET_a monthly time-series were used to assess the spatial and temporal ET_a dynamics for the Sindh canal commands for the 2000–2018 period. Figure 4-9 shows the spatial characteristics of mean annual, mean Kharif (April to September) and mean Rabi (October to March) ET_a, respectively. All maps are shown in a similar linear scale colour map for comparative purposes. In terms of annual ET_a means, large extents of irrigated areas within canal commands exceed 600 mm/y, and there are areas that exceed 1000 mm/y, particularly in canal commands in SRWN and SCWN. In part of these areas, ET_a exceeds 600 mm during Kharif. Lower mean annual and Kharif ET_a occur in canal commands in SCWS and SRWS, where annual means are generally around 900 mm/y and Kharif ET_a is generally 100 to 200 mm lower (around 400 mm to 600 mm) than in canal commands in SRWN and SCWN. On the other hand, there are areas in canal commands in both SRWN and SCWN with ET_a values exceeding 400 mm during Rabi, whereas most irrigated areas in canal commands in SCWS and SRWS are between 300 mm and 400 mm.

For further analysis, canal commands were grouped into larger canal command areas that are supplied from barrages in Sindh (see Figure 4-9a) and also by ACZs. Figure 4-10 shows the mean seasonal averages for the individual canal commands grouped by ACZs. The canal commands in BRW and SRWN (in blue, Figure 4-10)

have higher Kharif (492 mm/y) and Rabi (362 mm/y) ETa, respectively, than the SCWN and SRWS (in orange, 474 and 340 mm/y for Kharif and Rabi, respectively), and SCWN and SCWS (in green, 456 and 331 mm/y for Kharif and Rabi, respectively). In BRW and SRWN (in blue), the Rice canal command (51 in Figure 4-9) had the highest mean ET_a in both seasons, with 572 mm and 495 mm, for Kharif and Rabi respectively. Conversely, the Pat Feeder canal command (44 in Figure 4-9) had the lowest ET_a in Kharif (407 mm) and Desert canal command (45 in Figure 4-9) in Rabi (397 mm). In canal commands SCWN and SRWS (in orange), the Khairpur West (50 in Figure 4-9)) canal command had the highest mean ET_a in both seasons, with 572 mm and 495 mm, for Kharif and Rabi respectively. In canal commands SCWN and SCWS (in green), the Nara canal command (56 in Figure 4-9) had the highest mean ET_a in both seasons, with 468 mm and 342 mm, for Kharif and Rabi respectively.

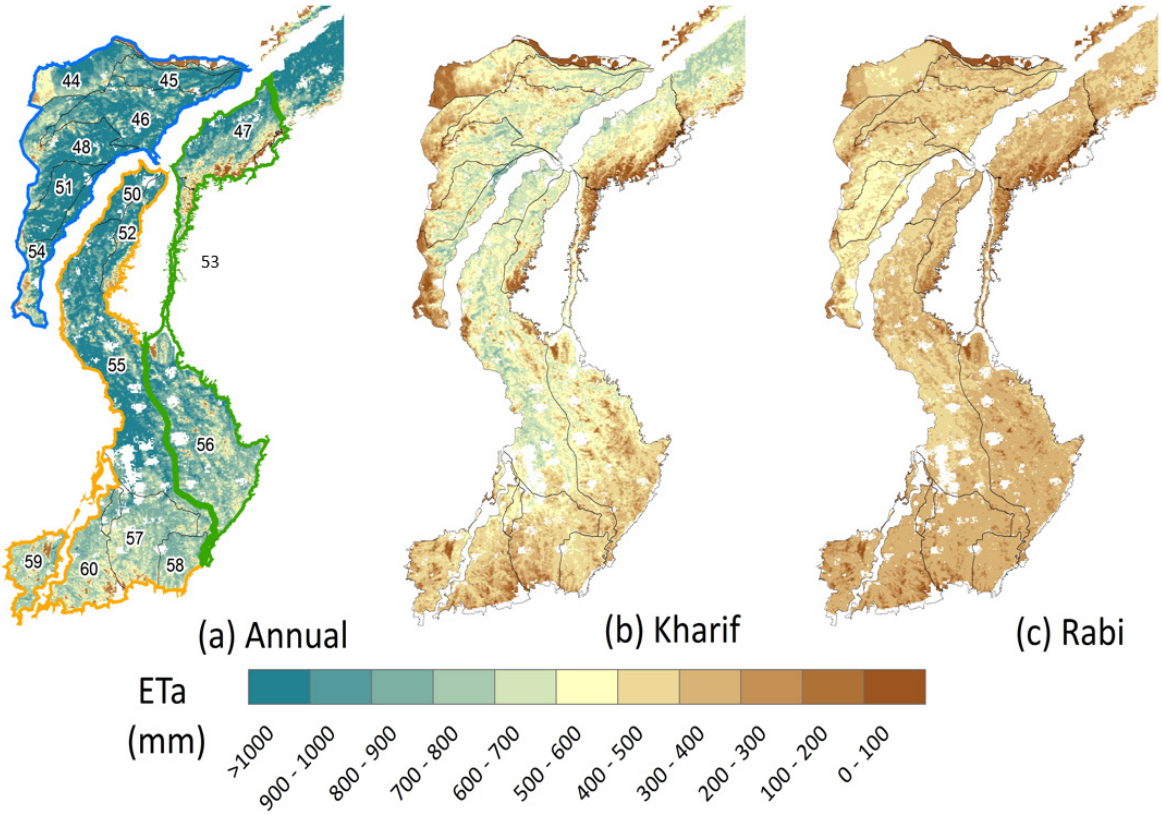

Figure 4-9 Spatial ET_a characteristics for the 2000–2018 period in the lower IBIS including: (a) mean annual ET_a, (b) mean Kharif (April to September) ET_a and (b) mean Rabi (May to October) ET_a. Canal command boundaries are shown in black. Note: the ID numbers in (a) depict a canal order ascending from north to south. A summary of canal commands and identification number can be found in Appendix A

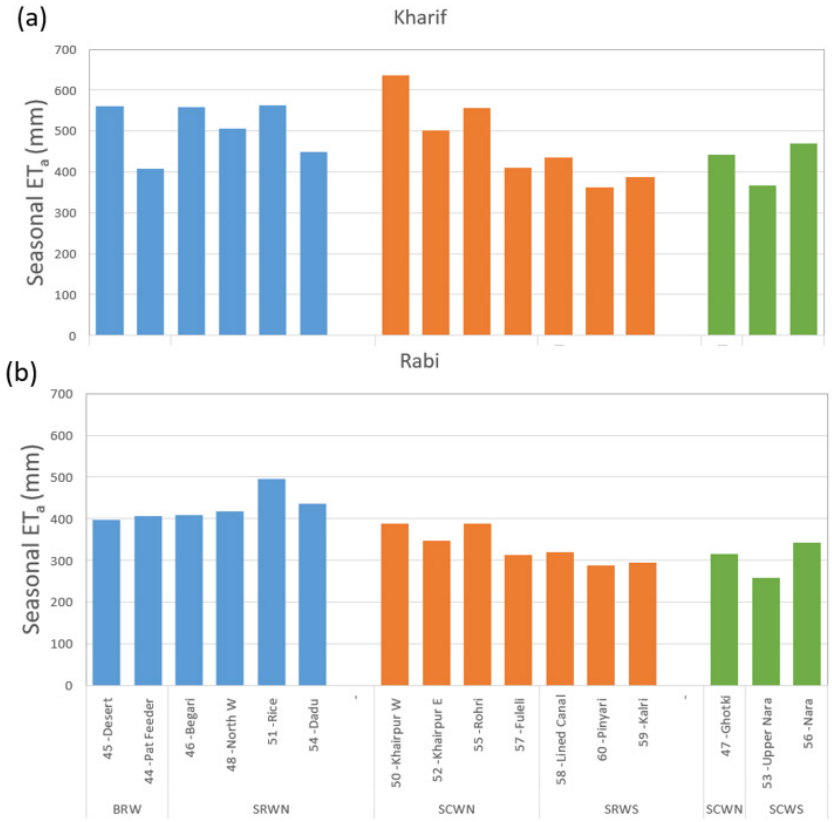

Figure 4-10 Mean seasonal (2000–2018 period) ETa aggregated for canal commands in the lower IBIS: (a) Kharif (April to October) and Rabi (November to March). Note: the ID numbers in (a) depict a canal order ascending from north to south, canal commands are colour coded to denote canals sharing the same surface water supply source

The grouped canal commands per ACZs exhibit seasonal variability on a year-to-year basis (Figure 4-11). Canal commands in SCWN and SCWS ACZs (green) had consistently less ET_a (about 10% on average) that the other two groups before the hydrologic year 2011–2012, particularly during Kharif. The situation changed after 2011–2012, where Kharif values in canal commands in SCWN and SCWS have come closer (about 3% less on average) to ET_a in canal commands BRW and SRWN and SCWN and SRWS, potentially indicating improvement in cropping conditions in canal commands in SCWN and SCWS. It is also noted that the input ET_0 data used for after 2013 came from a global model, rather than the locally interpolated ET_0 data used until 2013. Although great care has been taken in providing robust ET_0 time-series after 2013 using a per-pixel bias correction and ensuring consistency, it was not ascertained what the contributions of input ET_0 or VIs are in driving the changes after 2013.

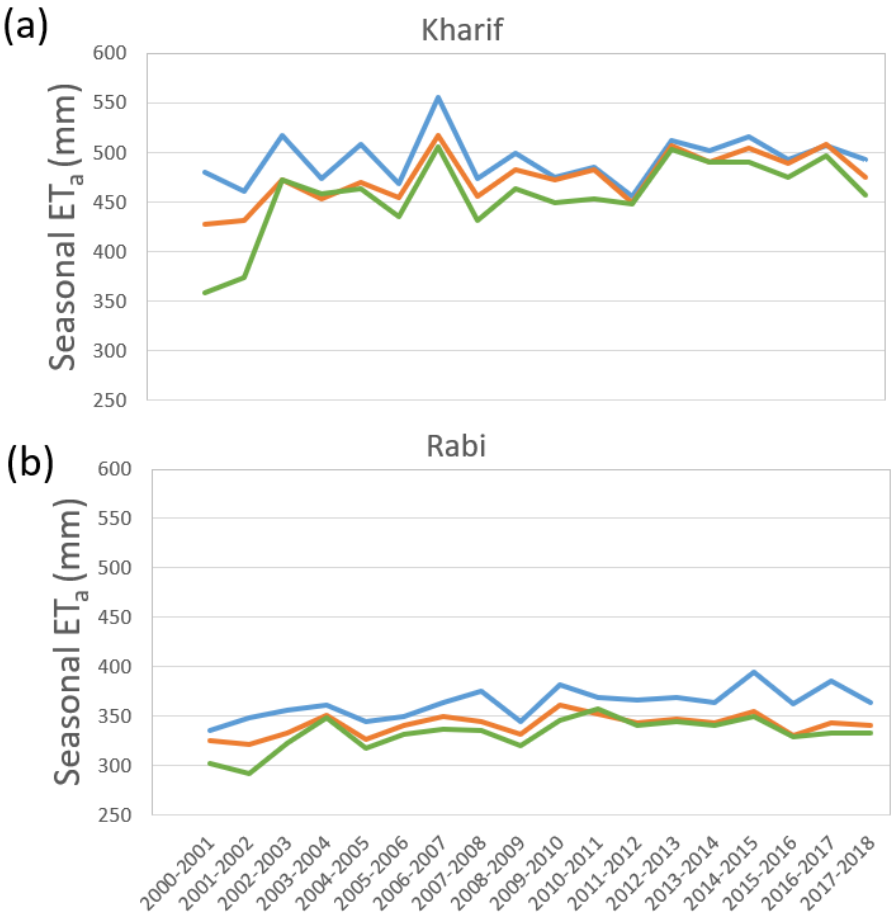

Figure 4-11 Kharif and Rabi ET_a hydrologic year (April to March) time-series from 2000 to 2018, aggregated for canal commands in the lower IBIS. Note: canal commands are grouped by colour to denote canals sharing the same surface water supply source

5 Summary and conclusion

The CMRSET (CSIRO MODIS ReScaled EvapoTranspiration) ET_a algorithm was implemented from 2000 to 2018 at 10-day temporal and 500 m spatial resolution in the Indus Basin Irrigation System (IBIS). Composites of daily MODIS data were aggregated to 10-day means to estimate two vegetation indices, the Enhanced Vegetation Index (EVI) and Global Vegetation Moisture Index (GVMI). Both indices are complementary: when EVI is low and GVMI is high, CMRSET can detect and estimating open water ET_a. This makes the algorithm useful for estimating ET_a under flood irrigation conditions. The indices were pre-processed and downloaded from Google Earth Engine, which facilitates pre-processing by minimising the effects of cloud cover and nulls.

CMRSET estimates were evaluated against the remotely sensed algorithms SEBAL and ET_{Look} at pixel and canal command scales, and against *in situ* Bowen ratio ET_a measurements at pixel scale. Generally, CMRSET compared well against both datasets, both in terms of magnitude and temporal patterns. CMRSET agreed better with SEBAL. For ET_{Look}, whilst the temporal patterns were well captured, the resulting magnitudes seem to be mixed, with 14 out of 56 canal commands having a positive percentage bias larger than 30%.

CMRSET ET_a estimates were also assessed against two *in situ* Bowen ratio surface energy balance ET_a measurements. For both locations, CMRSET had good agreement for both temporal patterns and magnitude.

The similarity of spatial and temporal patterns of actual evapotranspiration between CMRSET and the existing remotely sensed products gives confidence in its use for some applications. A companion report that assesses future scenarios impact on irrigated agriculture uses the remotely sensed ET_a products for scenario exploration and shows that they can be used with confidence for assessing changes in the water balance. However, the differences in actual values of the various methods suggests that care is required in the use of ET_a for quantitative water assessment or water balance analyses that uses absolute values, such as the assessment of volumes of groundwater that may be extracted sustainably.

The ET_a monthly time-series were used to assess spatial and temporal ET_a dynamics for the Sindh Province and for 16 canal commands therein for the 2000–2018 period. The assessment was performed annually (hydrologic year starting in April and finishing in March the next year) for the wet summer Kharif (April to September) season and for the dry winter Rabi (October to March). The assessment showed that ET_a in most irrigated areas within canal commands exceeded 600 mm/y, with areas that exceed 1000 mm/y, particularly in rice canal command areas. Lower mean annual and Kharif ET_a occur in cotton and rice canal commands in the south, with around 400 mm to 500 mm (about 100 to 200 mm less than in the canal commands more to the north). On the other hand, during Rabi, ET_a in most irrigated areas exceeded 300 mm.

These ET_a time-series provide the first long-term (>15 years) consistent ET_a time-series for the IBIS at spatial and temporal resolutions that are useful to assess irrigation systems at the canal command scale. CMRSET can be implemented straightforwardly using freely available data and processing through Google Earth Engine. CMRSET requires only multi-temporal satellite optical data to estimate a crop factor and climate data to estimate potential evapotranspiration and the product of these provides ET_a, both continuously updated and available through Google Earth Engine. This can enhance opportunities for monitoring irrigation dynamics and the assessment of structural and policy improvements in the IBIS.

Appendix A Assessed canal commands in the IBIS

A.1 Comparison of CMRSET ET_a against ET_{Look}

Table A-1 presents the summary for results for the comparison between CMRSET and ET_{Look} ET_a for the calendar year 2007 for each of the 56 canal commands assessed in this report.

Table A-1 Canal command characteristics, corresponding Agro-Climatic Zone (ACZ) and statistics of the CMRSET and ETLook comparison. Statistics include the Pearson's correlation coefficient (r), percentage bias, root mean square differences (RMSD) and the pixel-by-pixel spatial r

ID	Name	ACZ	Area (km^2)	ET_{Look} 2007 (mm/y)	CMRSET '07 (mm/y)	r	% Bias	RMSD	r spatial
1	Abazai	KPKS	374	776	1116	0.99	30.4	31.7	0.50
2	Upper Swat	KPKS	1474	881	1095	0.99	19.6	20.2	0.43
3	Warsak LB	KPKS	59	823	947	0.97	13.0	14.7	0.82
4	Doada LB	KPKS	156	821	1188	1.00	30.9	33.2	-0.05
5	L Swat	KPKS	822	772	1151	0.99	33.0	34.9	0.27
6	Kabul River	KPKS	581	896	1087	0.98	17.6	18.6	0.57
7	Pehur	KPKS	229	856	1062	0.99	19.4	19.2	0.73
8	Warsak	KPKS	549	574	710	0.96	19.1	13.8	0.94
9	Terbela	KPKS	275	665	874	0.95	23.9	20.3	0.77
10	Shah Joe	KPMW	63	568	885	0.94	35.7	30.2	0.76
11	Landi Dak	KPMW	180	486	843	0.93	42.3	34.0	0.74
12	Central Bannu	KPMW	535	425	774	0.91	45.0	32.6	0.83
14	U Jehlum	PSW	2856	1119	1092	0.95	-2.5	15.8	0.70
15	Marala Ravi	PRW	868	965	1105	0.97	12.7	15.4	0.03
16	L Jehlum	PSW	7341	897	1008	0.99	11.0	11.2	0.72
17	Raya	PRW	2190	917	1109	0.96	17.4	19.2	0.49
18	U Chenab	PRW	4649	1013	1112	0.97	8.9	13.0	0.40
19	CR BC-KP	KPMW	1607	453	1012	0.79	55.2	49.8	0.70
20	Thal	PMW	12026	359	680	0.92	47.2	27.9	0.89
21	Jhang	PRW	7432	985	1019	0.97	3.3	10.1	0.70
23	Gugera	PRW	8721	1088	1100	0.98	1.0	11.5	0.71
24	Bari Doab	PRW	3532	985	1080	0.97	8.8	12.0	0.68
25	CR BC-P	PCWW	1178	293	764	0.78	61.7	41.1	0.82
26	U Dipalpur	PRW	1634	1023	1130	0.98	9.5	12.7	0.85
27	U Rangpur	PCWW	1071	715	1039	0.96	31.2	28.5	0.86
28	Haveli	PSW	780	933	1054	0.98	11.4	11.7	0.91
29	Karanga	PSW	176	748	906	0.98	17.5	14.5	0.95

ID	Name	ACZ	Area ($km^{2)}$	ET_{Look} 2007 (mm/y)	CMRSET '07 (mm/y)	r	% Bias	RMSD	r spatial
30	L Dipalpur	PCWE	2770	1105	1157	0.98	4.5	11.5	0.73
31	L Bari Doab	PCWE	7889	1144	1125	0.99	-1.7	8.3	0.76
32	U Pakpattan	PCWE	4397	1113	1160	0.99	4.0	7.5	0.53
33	Sidhnai	PCWW	3464	1137	1181	0.99	3.8	7.3	0.73
34	Forwah	PCWE	2004	881	1123	0.97	21.6	21.4	0.66
35	L Rangpur	PCWW	509	859	1073	0.97	19.9	19.1	0.88
36	Muzafffargarh	PCWW	4166	855	1078	0.94	20.7	21.2	0.81
37	L Mailsi Pakpattan	PCWE	4662	1143	1163	0.97	1.8	12.1	0.73
38	Sadiqia	PCWE	5068	543	938	0.96	42.1	34.3	0.81
39	Dera GK	PCWW	5437	711	1042	0.86	31.7	32.0	0.89
40	Bahawal	PCWE	4356	646	918	0.94	29.6	24.2	0.86
41	Abbasia	PCWW	1416	521	780	0.95	33.2	22.6	0.85
42	Panjnad	PCWW	6082	1039	1200	0.95	13.4	18.6	0.73
44	Pat Feeder	BRW	3067	1026	882	0.89	-16.3	24.3	0.93
45	Desert	BRW	1798	945	898	0.94	-5.2	14.9	0.93
46	Begari	SRWN	4533	1057	891	0.94	-18.6	20.7	0.91
47	Ghotki	SCWN	4818	639	879	0.90	27.3	23.3	0.81
48	North W	SRWN	4028	938	758	0.94	-23.8	21.3	0.98
50	Khairpur W	SCWN	1169	1060	1187	0.98	10.7	12.4	0.65
51	Rice	SRWN	2244	1209	1085	0.92	-11.5	24.2	0.94
52	Khairpur E	SCWN	1940	579	955	0.90	39.4	33.0	0.82
53	Upper Nara	SCWS	1355	117	507	0.82	77.0	34.1	0.76
54	Dadu	SRWN	2550	738	801	0.90	7.9	11.8	0.93
55	Rohri	SCWN	11621	972	1086	0.90	10.5	13.3	0.82
56	Nara	SCWS	9641	574	844	0.68	32.1	25.4	0.78
57	Fuleli	SRWS	4227	797	719	0.83	-10.9	12.9	0.91
58	Lined Canal	SRWS	2143	482	582	0.68	17.1	13.4	0.89
59	Kalri	SRWS	2799	361	506	0.75	28.5	13.2	0.90
60	Pinyari	SRWS	3904	584	558	0.79	-4.6	9.0	0.90

A.2 Comparison of CMRSET ET_a against SEBAL

Summary of results for the comparison between CMRSET and SEBAL ET_a for the year (October to September) 2004–2005 for each of the 40 canal commands for which SEBAL was available (Table A-2).

Table A-2 Canal command characteristics, corresponding Agro-Climatic Zone (ACZ) and statistics of the CMRSET and SEBAL comparison. Statistics include the Pearson's correlation coefficient (r), percentage bias, root mean square differences (RMSD) and the pixel-by-pixel spatial r.

Order	Name	ACZ	Area (km^2)	SEBAL 0405 (mm/y)	CMRSET 0405 (mm/y)	r	% Bias	RMSD	r spatial
1	Abazai	KPKS	374	806	871	0.82	7.5	21.3	0.71
2	Upper Swat	KPKS	1474	812	848	0.91	4.3	13.8	0.60
3	Warsak LB	KPKS	59	793	767	0.88	-3.4	16.1	0.47
4	Doada LB	KPKS	156	918	948	0.78	3.1	26.0	0.11
5	L Swat	KPKS	822	885	928	0.80	4.7	23.2	0.36
6	Kabul River	KPKS	581	909	901	0.88	-0.9	16.9	0.32
7	Pehur	KPKS	229	847	823	0.94	-3.0	10.8	-0.25
8	Warsak	KPKS	549	731	695	0.94	-5.2	9.4	0.90
9	Terbela	KPKS	275	743	694	0.82	-7.0	16.7	0.53
10	Shah Joe	KPMW	63	834	742	0.97	-12.5	14.6	0.29
11	Landi Dak	KPMW	180	696	684	0.92	-1.8	11.9	0.79
12	Central Bannu	KPMW	535	696	692	0.95	-0.5	9.8	0.94
14	U Jehlum	PSW	2856	866	889	0.87	2.5	19.9	0.20
15	Marala Ravi	PRW	868	924	864	0.90	-7.0	22.4	0.10
16	L Jehlum	PSW	7341	802	837	0.89	4.1	14.9	0.60
17	Raya	PRW	2190	948	853	0.88	-11.0	21.2	0.18
18	U Chenab	PRW	4649	921	877	0.87	-4.9	20.5	0.17
19	CR BC-KP	KPMW	1607	774	765	0.94	-1.2	10.6	0.79
20	Thal	PMW	12026	420	576	0.85	27.1	15.6	0.87
21	Jhang	PRW	7432	760	826	0.92	8.0	12.6	0.70
23	Gugera	PRW	8721	831	873	0.91	4.8	13.9	0.38
24	Bari Doab	PRW	3532	863	851	0.88	-1.4	18.1	0.49
25	CR BC-P	PCWW	1178	566	585	0.78	3.2	12.8	0.71
26	U Dipalpur	PRW	1634	911	897	0.84	-1.6	21.9	0.71
27	U Rangpur	PCWW	1071	836	871	0.91	4.0	13.6	0.65
28	Haveli	PSW	780	884	893	0.90	1.1	16.4	0.70
29	Karanga	PSW	176	846	818	0.91	-3.5	16.7	0.90
30	L Dipalpur	PCWE	2770	921	902	0.85	-2.1	21.4	0.70
31	L Bari Doab	PCWE	7889	844	905	0.86	6.8	17.6	0.64
32	U Pakpattan	PCWE	4397	861	908	0.75	5.2	23.5	0.42
33	Sidhnai	PCWW	3464	875	979	0.86	10.6	18.6	0.54

Order	Name	ACZ	Area (km^2)	SEBAL 0405 (mm/y)	CMRSET 0405 (mm/y)	r	% Bias	RMSD	r spatial
34	Forwah	PCWE	2004	802	845	0.72	5.1	22.7	0.33
35	L Rangpur	PCWW	509	907	927	0.92	2.3	14.7	0.73
36	Muzafffargarh	PCWW	4166	777	886	0.86	12.3	17.4	0.84
37	L Mailsi Pakpattan	PCWE	4662	798	902	0.66	11.5	26.7	0.70
38	Sadiqia	PCWE	5068	508	704	0.63	27.8	23.8	0.78
39	Dera GK	PCWW	5437	754	812	0.72	7.2	21.3	0.85
40	Bahawal	PCWE	4356	541	718	0.54	24.7	25.3	0.87
41	Abbasia	PCWW	1416	454	621	0.76	26.8	18.6	0.94
42	Panjnad	PCWW	6082	749	942	0.81	20.5	25.3	0.82

References

Ahmad MUD, Bastiaanssen WGM, Feddes RA. 2002. Sustainable use of groundwater for irrigation: A numerical analysis of the subsoil water fluxes. Irrigation and Drainage 51: 227-41

Ahmad MD, Gamage N, Vithanage J, Masih I, Muthuwatte L, Gunasinghe S, Hussain A. 2008. Assessing the impact of physical and management interventions through RS/GIS tools on irrigation system performance in Punjab Pakistan (Final Report 2008) Colombo, Sri Lanka: International Water Management Institute.

Ahmad MD, Stewart JP, Peña-Arancibia JL, Kirby JM. 2020a. Sindh water outlook: Impacts of climate change, dam sedimentation and urban water supply on irrigated agriculture. Technical report. Sustainable Development Investment Portfolio project. CSIRO, Australia.

Ahmad MD, Stewart JP, Peña-Arancibia JL, Kirby JM. 2020b. Sindh Water Outlook: Impacts of Climate Change, Dam Sedimentation and Urban Water Supply on Irrigated Agriculture. Sustainable Development Investment Portfolio (SDIP) project. CSIRO, Australia.

Ahmad MD, Turral H, Nazeer A. 2009. Diagnosing irrigation performance and water productivity through satellite remote sensing and secondary data in a large irrigation system of Pakistan. Agricultural Water Management 96: 551-64

Archer DR Forsythe N, Fowler HJ, Shah SM. 2010. Sustainability of water resources management in the Indus Basin under changing climatic and socio-economic conditions. Hydrology and Earth System Sciences, 14, 1669-1680

Barron OV, Emelyanova I, Van Niel TG, Pollock D, Hodgson G. 2014. Mapping groundwater-dependent ecosystems using remote sensing measures of vegetation and moisture dynamics. Hydrological Processes 28: 372-85

Bastiaanssen WGM, Cheema MJM, Immerzeel WW, Miltenburg IJ, Pelgrum H. 2012. Surface energy balance and actual evapotranspiration of the transboundary Indus Basin estimated from satellite measurements and the ETLook model. Water Resources Research 48

Ceccato P, Flasse S, Gregoire JM. 2002. Designing a spectral index to estimate vegetation water content from remote sensing data-Part 2. Validation and applications. Remote Sensing of Environment 82: 198-207

Charles SP. 2016. Hydroclimate of the Indus - synthesis of the literature relevant to Indus Basin hydroclimate processes, trends, seasonal forecasting and climate change. CSIRO Sustainable Development Investment Portfolio project. CSIRO Land and Water, Australia. 48pp

Cheema MJM. 2012. Understanding water resources conditions in data scarce river basins using intelligent pixel information: Transboundary Indus Basin (Doctoral Thesis). Technische Universiteit, Delft.

Condon M, Kriens D, Lohani A, Sattar E. 2014. Challenge and response in the Indus Basin. Water Policy 16: 58-86

FAO and IHE Delft. 2019. WaPOR quality assessment. Technical report on the data quality of the WaPOR FAO database version 1.0. Rome. 134 pp. http://www.fao.org/3/ca4895en/ca4895en.pdf

Gorelick N et al. 2017. Google Earth Engine: Planetary-scale geospatial analysis for everyone. Remote Sensing of Environment, 202: 18-27. DOI:10.1016/j.rse.2017.06.031

Guerschman JP, Van Dijk A, Mattersdorf G, Beringer J, Hutley LB, et al. 2009. Scaling of potential evapotranspiration with MODIS data reproduces flux observations and catchment water balance observations across Australia. Journal of Hydrology 369: 107-19

Hargreaves GH. 1974. Estimation of Potential and Crop Evapotranspiration. Transactions of the ASAE 17: 701-4

Huete A, Didan K, Miura T, Rodriguez EP, Gao X, Ferreira LG. 2002. Overview of the radiometric and biophysical performance of the MODIS vegetation indices. Remote Sensing of Environment 83: 195-213

Hutchinson MF, Xu T. 2013. ANUSPLIN Version 4.4 User Guide. Fenner School of Environment and Society, Australian National University, Canberra. http://fennerschool.anu.edu.au/files/anusplin44.pdf

Kirby M, Ahmad MUD, Mainuddin M, Khaliq T, Cheema MJM. 2017. Agricultural production, water use and food availability in Pakistan: Historical trends, and projections to 2050. Agricultural Water Management 179: 34-46

Paca VHD, Espinoza-Davalos GE, Hessels TM, Moreira DM, Comair GF, Bastiaanssen WGM. 2019. The spatial variability of actual evapotranspiration across the Amazon River Basin based on remote sensing products validated with flux towers. Ecological Processes 8

Peña-Arancibia JL, Mainuddin M, Kirby JM, Chiew FHS, McVicar TR, Vaze J. 2016. Assessing irrigated agriculture's surface water and groundwater consumption by combining satellite remote sensing and hydrologic modelling. Science of the Total Environment 542: 372-82

Peña-Arancibia JL, Mainuddin M, Ahmad M, Hodgson G, Khandakar F, Ticehurst C, Maniruzzaman M, Golam M, Kirby JM. 2019. Groundwater use and rapid irrigation expansion in a changing climate: hydrological drivers in one of the world's food bowls. Journal of Hydrology. https://doi.org/10.1016/j.jhydrol.2019.124300.

Peña-Arancibia JL, McVicar TR, Paydar Z, Li L, Guerschman JP, et al. 2014. Dynamic identification of summer cropping irrigated areas in a large basin experiencing extreme climatic variability. Remote Sensing of Environment 154: 139-52

Reichle RH, Koster RD. 2004. Bias reduction in short records of satellite soil moisture. Geophysical Research Letters 31 http://dx.doi.org/Artn L1950110.1029/2004gl020938.

Rodell M, Houser PR, Jambor U, Gottschalck J, Mitchell K, et al. 2004. The Global Land Data Assimilation System. Bulletin of the American Meteorological Society 85. https://journals.ametsoc.org/doi/10.1175/BAMS-85-3-381

Silberstein RP, Dawes WR, Bastow TP, Byrne J, Smart NF. 2013. Evaluation of changes in post-fire recharge under native woodland using hydrological measurements, modelling and remote sensing. Journal of Hydrology 489: 1-15

Stewart JP, Podger GM, Ahmad MD, Shah MA, Bodla H, Khero Z, Rana MKI. 2018. Indus River System Model (IRSM) – a planning tool to explore water management options in Pakistan: model conceptualisation, configuration and calibration. August 2018. Technical report. South Asia Sustainable Development Investment Portfolio (SDIP) Project. CSIRO, Australia. 155p

Van Dijk AIJM, Bacon D, Barratt D, Crosbie R, Daamen C, et al. 2011. *Design and development of the Australian Water Resources Assessment system*. Presented at Proceedings, Water Information Research and Development Alliance Science Symposium, August 2011. Melbourne. Available from http://www.csiro.au/WIRADA-Science-Sympsosium-Proceedings

Yin JF, Zhan XW. 2018. Impact of Bias-Correction Methods on Effectiveness of Assimilating SMAP Soil Moisture Data into NCEP Global Forecast System Using the Ensemble Kalman Filter. *Ieee Geoscience and Remote Sensing Letters* 15: 659-63

Zhou J, Jia L, Menenti M. 2015. Reconstruction of global MODIS NDVI time series: Performance of Harmonic ANalysis of Time Series (HANTS). Remote Sensing of Environment 163: 217-28

As Australia's national science agency and innovation catalyst, CSIRO is solving the greatest challenges through innovative science and technology.

CSIRO. UNLOCKING A BETTER FUTURE FOR EVERYONE

FOR FURTHER INFORMATION

CSIRO Land and Water
Dr Jorge Luis Pena Arancibia
+61 2 6246 5711
jorge.penaarancibia@csiro.au
www.csiro.au/

Dr Mobin-ud-Din Ahmad
Project Leader – Indus SDIP Pakistan
+61 2 6246 5936
mobin.ahmad@csiro.au
research.csiro.au/sdip/projects/indus/

1300 363 400
+61 3 9545 2176
CSIROEnquiries@csiro.au
www.csiro.au